AGU ADVANCING EARTH AND SPACE SCIENCE

Geophysical Research Letters

RESEARCH LETTER

10.1029/2020GL090641

New Precise Dating of the India-Asia Collision in the Tibetan Himalaya at 61 Ma

Wei An[1,2], **Xiumian Hu**[2], **Eduardo Garzanti**[3], **Jian-Gang Wang**[4], **and Qun Liu**[2]

[1]School of Resources and Environmental Engineering, Hefei University of Technology, Hefei, China, [2]School of Earth Sciences and Engineering, State Key Laboratory of Mineral Deposits Research, Nanjing University, Nanjing, China, [3]Department of Earth and Environmental Sciences, Università di Milano-Bicocca, Milano, Italy, [4]State Key Laboratory of Lithospheric Evolution, Institute of Geology and Geophysics, Chinese Academy of Sciences, Beijing, China

Key Points:

- Sandstones derived first from India and next from Asia constrain India-Asia collision onset
- The India-Asia provenance reversal is bracketed between 62.7 and 61 Ma in the Mubala section
- Subduction of the Indian continental margin beneath Asia began by 61 Ma

Supporting Information:

- Supporting Information S1
- Figure_S1
- Figure_S2
- Figure_S3
- Data Set S1

Correspondence to:

X. Hu,
huxm@nju.edu.cn

Citation:

An, W., Hu, X., Garzanti, E., Wang, J. G., & Liu, Q. (2021). New precise dating of the India-Asia collision in the Tibetan Himalaya at 61 Ma. *Geophysical Research Letters*, *48*, e2020GL090641. https://doi.org/10.1029/2020GL090641

Received 8 SEP 2020
Accepted 9 JAN 2021

Abstract

The timing of the India-Asia collision onset, essential to understanding the evolution of the Himalayan-Tibetan orogen, has been widely investigated through multidisciplinary approaches. Among these, the India to Asia provenance reversal (IAPR) documented in the Indian passive margin successions has proved to be most effective. We present integrated stratigraphic, sedimentological, and provenance data on Upper Cretaceous-Paleogene strata from the newly investigated Mubala section exposed south of the Yarlung-Zangbo suture zone (YZSZ) in southern Tibet, which preserves continuous deep-marine turbiditic and biogenic sedimentation on the distal Indian passive margin. Sandstone petrography, heavy minerals, detrital zircon geochronology and Hf isotopes, and detrital Cr-spinel geochemistry constrain the IAPR to later than 62.7 Ma (youngest zircon ages from the earliest Asian-derived sandstone) and by 61.0 ± 0.3 Ma (SIMS age of a tuffaceous layer ~30 m above this bed). The onset of intercontinental collision along the YZSZ began by 61 Ma.

Plain Language Summary

The India-Asia collision, ultimately leading to uplift of the Himalayan Mountains and Tibetan Plateau, has greatly influenced global climate and oceanic circulation. The timing of collision is essential to reconstruct the growth history of the Himalayan-Tibetan orogen and its environmental and paleogeographic effects. The change in sediment provenance documented along the Indian continental margin has proved to be a most effective method to constrain the timing of initial collision. We here report a newly-discovered sedimentary succession deposited onto the deep-marine edge of India, in which strata composed of detritus derived entirely from India are overlain by strata composed of detritus derived instead from Asia. This provenance change took place later than 62.7 million years ago (Ma; which is the age of the youngest group of zircons contained in the oldest sandstone derived from Asia) and 61.0 ± 0.3 Ma (which is the age of zircon crystals contained in a volcanic tuff found 30 m above the oldest Asian-derived sandstone). The Indian and Asian continents thus first came into direct contact by 61 Ma.

1. Introduction

The India-Asia collision induced rapid uplift of the Tibetan Plateau and affected global atmospheric and oceanic circulation through the Cenozoic (Z. An et al., 2001; Ravizza & Zachos, 2014). Geological records both in the western (Indus suture zone) and central-eastern Himalaya (Yarlung-Zangbo suture zone; YZSZ) indicate an early Paleogene collision event, interpreted as India colliding with either an intra-oceanic arc (e.g., Aitchison et al., 2007) or with Asia (e.g., Garzanti, 2008). Because no record of an oceanic basin still open after this collision event has ever been documented either in the central Himalaya to the south or in Tibet to the north, the latter hypothesis (DeCelles et al., 2014; Hu et al., 2016) is favored here.

Multidisciplinary approaches, including stratigraphy, paleomagnetism, and metamorphic petrology have been used to assess the timing of initial collision, a key point from which to start reconstructing the subsequent evolution of the Himalayan-Tibetan orogen and its global consequences (e.g., Beck et al., 1995; Ding et al., 2005; Leech et al., 2005; van Hinsbergen et al., 2012; Yin & Harrison, 2000). Previous studies documented that the India to Asia provenance reversal (IAPR) recorded in sandstones deposited on the Indian passive margin represents a fundamental clue to constrain the timing of initial collision (Garzanti et al., 1987; Hu, Garzanti, Moore, et al., 2015; Najman et al., 2017, 2010). The age of this major geological event has been pin-pointed in deep-water turbiditic successions as ~59–60 Ma (DeCelles et al., 2014; Hu, Garzanti, Moore, et al., 2015; Wang et al., 2011; Wu et al., 2014;), which is consistent with most available geological information excepting the too distant paleolatitude positions of India relative to Asia suggested by paleomagnetic evidence (van Hinsbergen et al., 2012; Yuan et al., 2021).

The Sangdanlin section in Tibet, south of the YZSZ, has been thoroughly studied for this purpose. The determination of nannofossil assemblages from strata ~100 m above the IAPR and of radiolarian assemblages both below and above the IAPR (Hu, Garzanti, Moore, et al., 2015), combined with detrital-zircon chronostratigraphy (directly above the IAPR; DeCelles et al., 2014; Wang et al., 2011; Wu et al., 2014) and zircon ages in a tuff layer ~510 m above the IAPR (DeCelles et al., 2014) have constrained the India-Asia collision onset as 59 ± 1 Ma (Hu, Garzanti, Moore, et al., 2015). All of these methods, however, are potentially subject to minor imprecision. The nannofossil-bearing beds and the tuff layer are younger than the IAPR, the time range of radiolarian biozones is not precisely determined, and stratigraphic or tectonic discontinuities may occur (Y. Li et al., 2007). Because the currently available information has been considered insufficient to establish the age of such a prominent geological event conclusively, we carried out further field work aimed at identifying stratigraphic sections suited to both constrain collision onset with improved accuracy and precision and to quantify its potential diachroneity along strike.

In this study, we provide new stratigraphic, petrographic, heavy-mineral, geochronological, and geochemical data from Upper Cretaceous-Paleogene strata exposed continuously in the newly discovered Mubala section south of the YZSZ in southern Tibet (Figures 1a and 1b). These new data constrain collision onset to have occurred by 61 Ma in the Mubala section, which thus preserves the earliest record of transition between Indian-passive-margin and Transhimalayan-trench sedimentation associated with the India-Asia collision documented to date.

2. Geological Setting

The Mubala section is located ~65 km southwest of Saga south of the YZSZ in Tibet (N 29°19′41″N, E 84°41′16 ″E; Figures 1a and 1b). The Transhimalayan arc-trench system (Hu et al., 2020; Orme et al., 2021) consists of the Gangdese magmatic arc, the Xigaze forearc basin hosting Aptian-Eocene marine to non-marine successions stratigraphically overlying the Xigaze forearc ophiolites, and an accretionary prism including mud- and serpentinite-matrix mélange (W. An et al., 2017; Metcalf & Kapp, 2017; Orme et al., 2014). To the south, the Tethyan Himalaya zone comprises Paleozoic to Eocene strata representing the northern Indian passive margin (Hu et al., 2012; Sciunnach & Garzanti, 2012; Willems et al., 1996).

3. Stratigraphy

The Mubala section (Figure 1c) was measured at bed-by-bed of detail and logged at 1:2500 scale (Figure 2a). The 330 m-thick siliciclastic succession conformably overlies dark gray siliceous shale interbedded with chert of the Jiabula Formation (Figures 2b and 2c) deposited on the distal shelf within the Tethyan Himalaya (X. Li et al., 2005). The succession can be subdivided into three parts with conformable stratigraphic contacts marking distinct lithological changes and correlating with the Denggang, Sangdanlin, and lower Zheya formations identified in the Sangdanlin section (DeCelles et al., 2014; Hu, Garzanti, Moore, et al., 2015; Wang et al., 2011; Figures 1c and Figure 2a).

The Denggang Formation (160 m-thick) is subdivided into three informal members in the Mubala section. The lower member (60 m-thick) consists of green siliceous shale passing upward to thick-bedded, medium to coarse-grained sandstone (Figure 1c1). The middle member (30 m-thick) consists of 0.1–1.5 m-thick, fine- to coarse-grained sandstone intercalated with siltstone (Figure 1c2). The upper member (70 m thick) consists of dark green, 0.1–0.6 m-thick, fine-grained sandstone beds (Figures 1c3 and 2d) interbedded with green/purple radiolarian chert and purple siliceous shale. The lower member correlates lithostratigraphically with Units 1–8 of the Sangdanlin section, whereas the middle and upper members correlate with Units 9–10 (DeCelles et al., 2014; Hu, Garzanti, Moore, et al., 2015). Sandstone beds display erosional base, flute casts, parallel or ripple lamination, and common intraclasts, indicating deposition from turbidity currents.

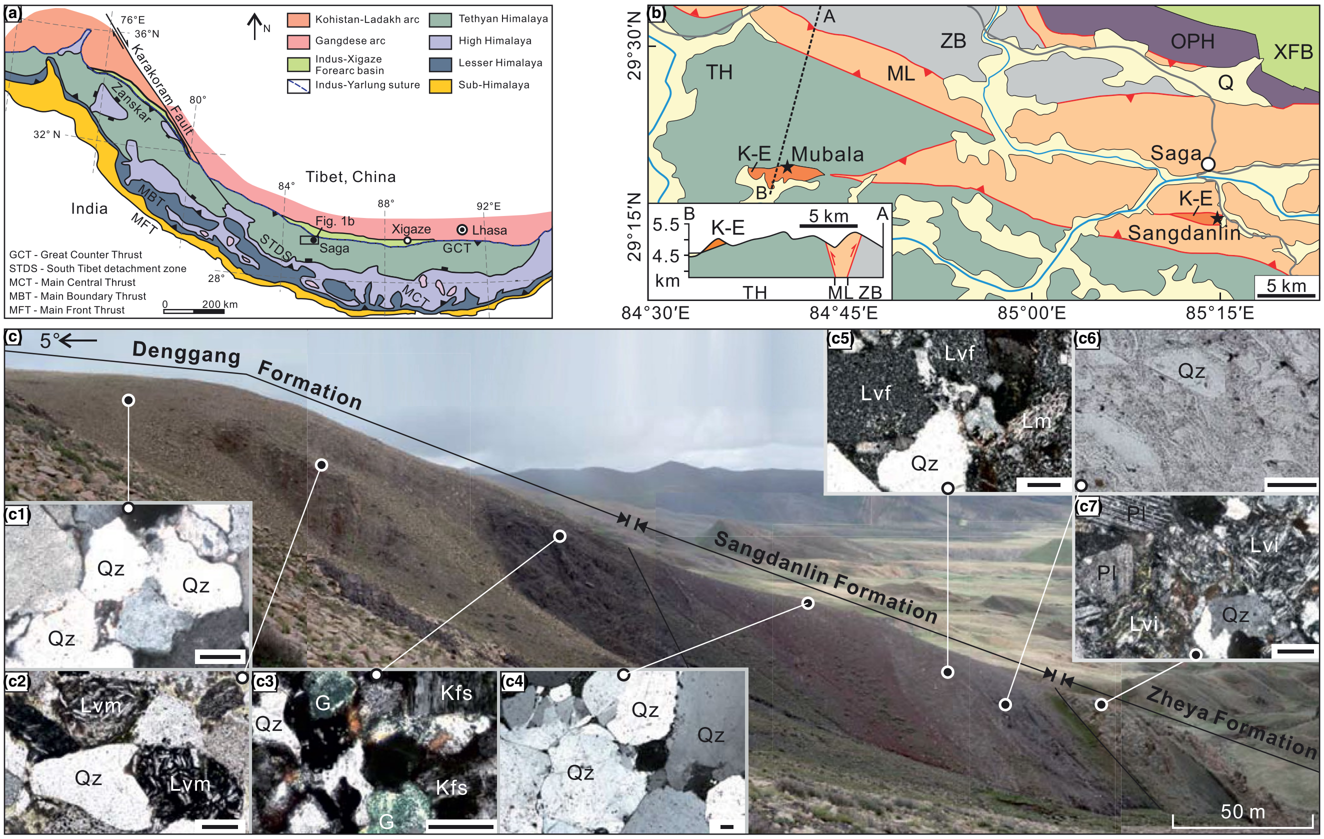

Figure 1. The Mubala section in southern Tibet (strata dip to the right and are more inclined than the slope): (a) geological sketch map of the southern Lhasa terrane and Himalayan belt; (b) simplified geological map and cross-section of the Saga area (based on Hu et al., 2016; Metcalf & Kapp, 2017; Pan et al., 2004, and own field observations) with locations of the Mubala and Sangdanlin sections shown by stars, ML, Xiukang complex; OPH, Ophiolites of the YZSZ; K-E, Cretaceous-Paleogene strata; Q, Quaternary; TH, Tethyan Himalaya; XFB, Xigaze forearc basin; ZB, Zhongba terrane; (c) panorama of the studied Mubala stratigraphic section including (older to younger): India-derived quartzose (c1) and quartzo-lithic basalticlastic (c2) sandstones of the lower and middle Denggang Formation; glaucony-bearing feldspatho-quartzose (c3) and quartzose (c4) sandstones of the upper Denggang and lower Sangdanlin formations; Asian-derived feldspatho-litho-quartzose volcaniclastic sandstones (c5) and interbedded tuff layers (c6) of the upper Sangdanlin Formation; and, sandstones of the Zheya Formation (c7). G, glaucony; Kfs, K-feldspar; Lm, metamorphic lithic grains; Lvm, Lvi, Lvf, mafic, intermediate and felsic volcanic lithic grains; Pl, plagioclase; Qz, quartz; 100 μm bar for scale.

Thick and coarse-grained beds in the lower and middle members were deposited by high-density flows, whereas thinner beds in the upper member document low-density flows intercalated with background biogenic radiolarian chert (Mutti, 1992).

The Sangdanlin Formation (120 m-thick) consists of two members in the Mubala section. The lower member (50 m-thick) includes purple siliceous shale intercalated with purple radiolarian chert and lenticular sandstone (Figures 1c4, and 2d). The upper member includes 30 m of thin- to medium-bedded, medium- to coarse-grained sandstone (Figures 1c5 and 2e) overlain by 40 m of purple siliceous shale intercalated with numerous thin-bedded tuff layers (Figures 1c6, and 2e). The lower member correlates lithostratigraphically with Units 11–13 of the Sangdanlin section, whereas the upper member is similar to Units 14–21 (DeCelles et al., 2014; Hu, Garzanti, Moore, et al., 2015). Radiolarian chert and siliceous shale indicate biogenic deposition at abyssal depths during periods of reduced clastic influx, possibly representing forebulge-top deposits isolated from detritus from both directions as those in the Sangdanlin section (DeCelles et al., 2014). Sandstone beds showing flute and groove casts, parallel and ripple lamination, graded-bedding, or erosional base indicate deposition from distal turbidity currents (Mutti, 1992).

The Zheya Formation (50 m) consists of thin- to thick-bedded, medium-grained to pebbly sandstones with upward-decreasing gray shale intercalations (Figure 1c7) in the Mubala section, corresponding lithostratigraphically to Units 22–26 of the Sangdanlin section (DeCelles et al., 2014; Hu, Garzanti, Moore, et al., 2015).

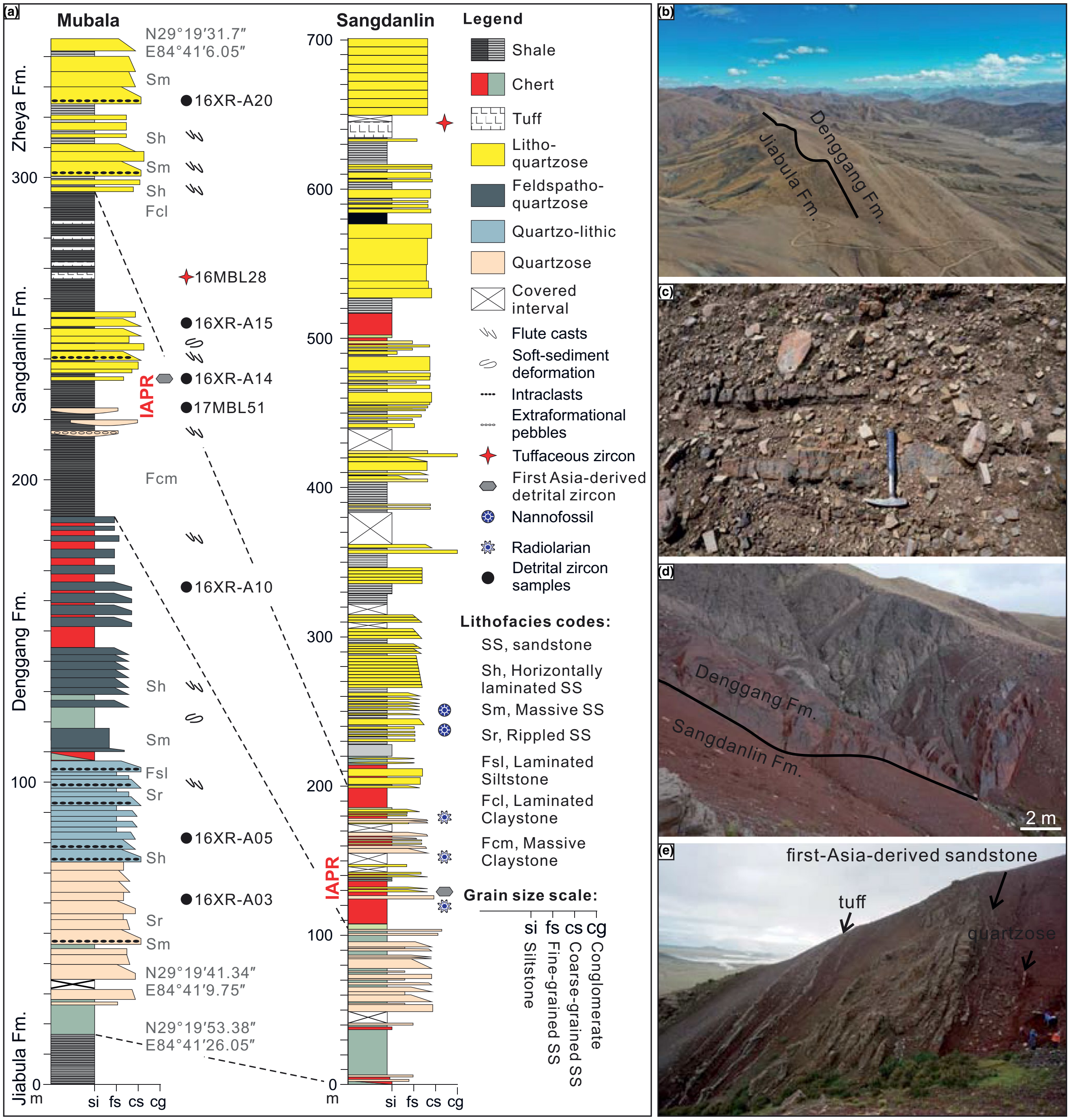

Figure 2. The Mubala section (a) and field photos (b–e): (a) stratigraphic column of the Mubala section correlated with the Sangdanlin section exposed ~60 km to the east (after DeCelles et al., 2014); (b) conformable contact between Upper Cretaceous Jiabula Formation and overlying Denggang Formation; (c) siliceous shales intercalated with chert in the Jiabula Formation; (d) conformable contact between Denggang and Sangdanlin formations; (e) first Asian-derived feldspatho-litho-quartzose sandstone in upper Sangdanlin Formation (overlying thin-bedded tuff to the left).

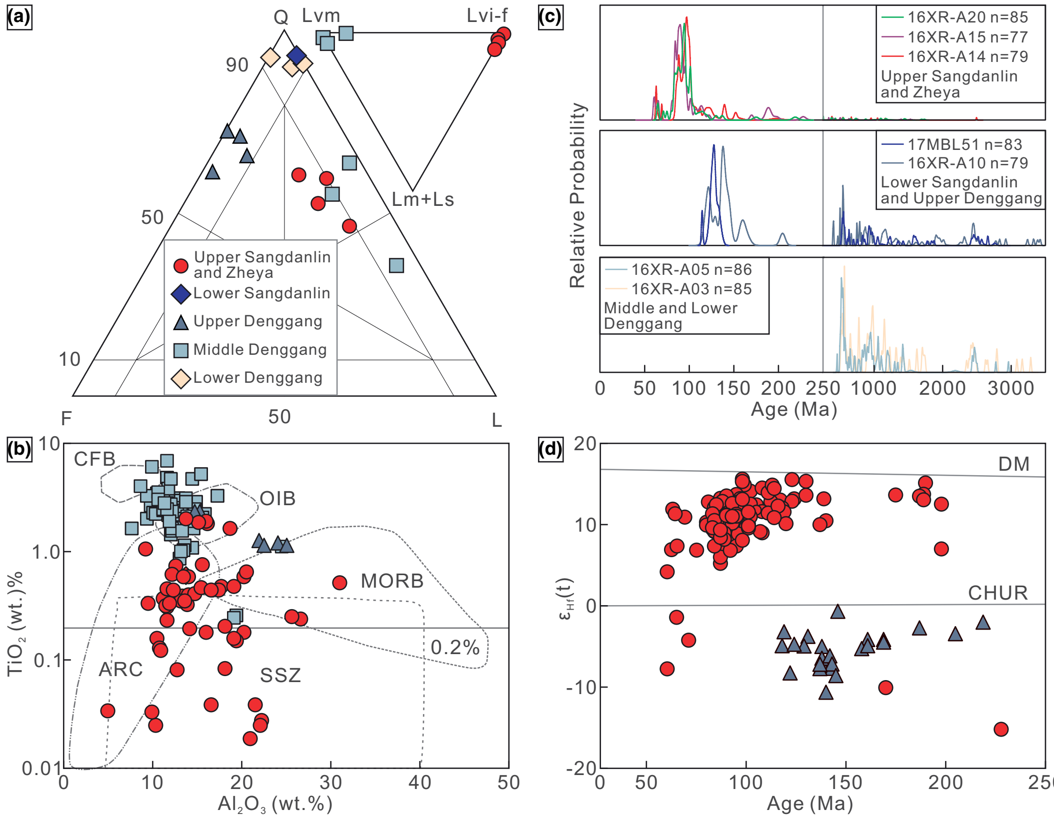

Figure 3. Provenance data from the Mubala section: (a) petrography. Compositional fields in the QFL plot (F, feldspars; L, lithic grains; Q, quartz) after Garzanti (2019). Lm + Ls, metamorphic and sedimentary lithic grains; Lvm and Lvi-f, mafic and intermediate + felsic volcanic lithic grains; (b) geochemistry of detrital Cr-spinel. Compositional fields after Kamenetsky et al. (2001): Arc, arc; CFB, continental-flood basalt; MORB, mid-ocean-ridge basalt; OIB, oceanic-island basalt; SSZ, supra-subduction-zone; (c) detrital zircon U-Pb age spectra; (d) Mesozoic zircon Hf isotopic signature. All data available in Tables S1–S4.

Parallel or ripple lamination, graded-bedding, erosional base, load or flute casts and intraclasts are common, suggesting deposition by high-density turbidity currents.

4. Methods and Sampling

15 sandstone samples collected throughout the Mubala section were point-counted following the Gazzi-Dickinson method (Ingersoll et al., 1984) and classified according to Garzanti (2019). Heavy-mineral analysis was conducted on nine of these samples. Cr-spinel was separated from five samples of the Denggang and Sangdanlin formations. Detrital zircon from seven samples yielded 574 concordant U-Pb ages, of which 237 Cenozoic-Mesozoic grains were analyzed for Hf isotopes. Thirty-six ages were obtained from the tuff in the upper Sangdanlin Formation. See supporting information for detailed analytical procedures and complete data sets.

5. Results

In the Denggang Formation, sandstones are quartzose in the lower member, litho-quartzose to quartzo-lithic basalticlastic in the middle member, and glaucony-bearing feldspatho-quartzose in the upper member (Figure 3a). In the Sangdanlin Formation, sandstones are quartzose in the lower member and feldspatho-litho-quartzose volcaniclastic in the upper member as in the overlying Zheya Formation (Figure 3a). Heavy minerals document an upward decrease in durable zircon, tourmaline, and rutile. Garnet and apatite characterize the Denggang and lower Sangdanlin formations, whereas epidote is dominant in the upper Sangdanlin and Zheya formations. Cr-spinel grains from the middle and upper Denggang Formation have higher TiO_2 content than those from the Sangdanlin Formation (Figure 3b).

Detrital zircon from the lower and middle Denggang Formation exhibits prominent age clusters at 500–570 Ma (peaks at ∼522 and ∼567 Ma) and 800–1,000 Ma (peak at ∼950 Ma) with subordinate older ages (Figure 3c). Detrital zircon from the upper Denggang and lower Sangdanlin formations displays similar age spectra, with an additional cluster at 115–150 Ma (peaks at ∼128 and 138 Ma) characterized by negative εHf(t) values (Figure 3d). In contrast, zircon grains from the upper Sangdanlin and Zheya formations yielded mainly Cenozoic-Mesozoic ages (Figure 3c), with clusters at 60–70 Ma and 80–120 Ma and mainly positive εHf(t) values (Figure 3d).

6. The India-Asia Provenance Reversal

Petrographic, heavy-mineral, and geochronological data document multistep changes in provenance through the Mubala section. Quartzose sandstones in the lower Denggang Formation were derived from cratonic interiors, whereas abundant basaltic detritus in the middle member was sourced from mafic lavas. Glaucony grains in the upper member were possibly formed authigenically in situ at the expense of weathered glassy volcanic fragments or resedimented from shallower-water sediments deposited during a stage of starved sedimentation (Garzanti & Hu, 2015). The Sangdanlin Formation documents a provenance change from quartzose sandstones derived from cratonic interiors in the lower member, to volcaniclastic sandstones with abundant plagioclase, K-feldspar, and epidote derived from a magmatic arc in the upper member.

These provenance interpretations are supported by detrital zircon ages, Hf isotopes and Cr-spinel geochemistry. The lower and middle Denggang sandstones contain common Paleozoic-Archean zircon grains, showing an age spectrum similar to pre-Cretaceous sandstones of the Tethyan Himalaya and northern India (Cawood et al., 2007; DeCelles et al., 2000). The upper Denggang and lower Sangdanlin sandstones are characterized by zircon grains yielding Early Cretaceous ages with negative εHf(t) values and Paleozoic-Archean ages, similar to the Cretaceous-Paleocene sandstones of the Tethyan Himalaya, derived ultimately from the Early Cretaceous intra-plate volcanics and recycled sediments in the northern India (DeCelles et al., 2014; Gehrels et al., 2011; Hu et al., 2010; Hu, Garzanti, & An, 2015). Cr-spinel grains have high TiO_2 content, similar to those in Tethyan Himalayan strata (Hu et al., 2014). In contrast, the upper Sangdanlin sandstones yielded zircon grains with predominant Cenozoic-Mesozoic ages and positive εHf(t) values, indicating provenance from the Gangdese magmatic arc (DeCelles et al., 2014; Hu, Garzanti, Moore, et al., 2015; Ji et al., 2009), supported by the low TiO_2 content in detrital Cr-spinel (Hu et al., 2014).

Quartzose sandstones in the lower Denggang Formation were derived from India. The transition to quartzo-lithic basalticlastic sandstones in the middle Denggang Formation testifies to the main outburst of Deccan volcanism close to the Cretaceous/Tertiary boundary (e.g., Chenet et al., 2007; J. Li et al., 2020). The further upward transition to the glaucony-bearing feldspatho-quartzose sandstones of the upper Denggang Formation and quartzose sandstones of the lower Sangdanlin Formation would be consistent with either deepening of erosion into Early Cretaceous volcanic and volcaniclastic rocks within northern India or with further recycling of Cretaceous-lower Paleocene Tethys Himalayan sandstones possibly uplifted and eroded during passage over the forebulge (DeCelles et al., 2018).

The most prominent provenance change (the IAPR), which represents a direct testimony of India-Asia collision onset (DeCelles et al., 2014), is documented between the lower and upper Sangdanlin Formation. In the Mubala section, the IAPR corresponds to an abrupt change from Indian-derived quartzose sandstones to feldspatho-litho-quartzose volcaniclastic turbidites derived from Asia. This is notably different from the Sangdanlin section, where Indian and Asian-derived turbidites are intercalated through much of the central part of the Sangdanlin Formation (Wang et al., 2011). Asian-derived detritus also varies between the two sections, K-feldspar being present in the Mubala section but lacking in the Sangdanlin section. This indicates different source areas along strike within the same magmatic arc, with more detritus from the plutonic core of the arc massif supplied to the Mubala section.

A maximum age constraint to the IAPR is provided by the youngest age cluster of detrital zircon contained in the first Asian-derived sandstone, displaying a prominent peak at 62.7 Ma (Figure 3b). A firmer age constraint is the SIMS age of 61.0 ± 0.3 Ma obtained from the tuff layer lying ∼30 m stratigraphically above the first Asian-derived sandstone (Figures 4a and 4b). The IAPR in the Mubala section is therefore

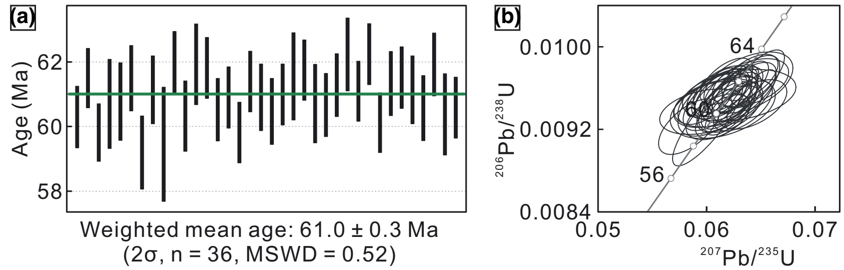

(c)

Section	Preserved position above IAPR (m)	Dating Method	Age (Ma)
Mubala	~30	TZ SIMS	61.0±0.3
	0	DZ LA-ICPMS	62.8±0.7[1]/62.7[2]
Sangdanlin	~510	TZ LA-MC-ICPMS/SIMS	58.5±0.6[3]/58.4±0.4[4]
	~100	Nannofossil	CNP7 (60.2-58.3)
	~20	Radiolarian	RP6 (60.2-56.9)
	0	DZ LA-ICPMS	60.4±3.2[1]/60.6[2]

Figure 4. Dating the IAPR with different methods: (a), (b) age plots for the tuff 30 m above the base of the upper Sangdanlin Formation, MSWD, mean squared weighted deviation; (c) comparison between chronostratigraphic data obtained from Mubala and Sangdanlin sections (after DeCelles et al., 2014; Hu, Garzanti, Moore, et al., 2015, and this study): DZ, detrital zircon; TZ, tuffaceous zircon; (1) weighted mean age for the youngest cluster of zircon grains; (2) peak age of the youngest cluster of zircon grains; (3) LA-MC-ICPMS zircon ages; (4) SIMS zircon ages. All data provided in Table S5.

robustly bracketed between 62.7 Ma and 61.0 ± 0.3 Ma. This age interval appears to be a bit older than the pre-58.5 Ma (DeCelles et al., 2014) and 59 ± 1 Ma (Hu, Garzanti, Moore, et al., 2015) estimate obtained from the Sangdanlin section. The discrepancy could be explained by the closer position of the Mubala tuff to the IAPR (~30 m above) than the Sangdanlin tuff (~510 m above; Figure 4c), or by the imprecision of zircon ages.

7. Timing of the India-Asia Collision Onset

The onset of continental collision is most aptly defined as the moment when the two opposite continental margins come into physical contact, continental subduction begins, and no oceanic lithosphere is left in between (Beck et al., 1995; DeCelles et al., 2014; Hu et al., 2016). Among the diverse methods proposed to pin-point the precise moment when the distal edge of the Indian continental began to subduct beneath Asia, the coupled stratigraphic/sediment-provenance approach has proved to be the most direct one, and consequently the most robust (e.g., Garzanti et al., 1987; Hu et al., 2016).

In this respect, the importance of the Mubala section resides in the fact that it rests stratigraphically on top of the Jiabula Formation, proving that deposition took place onto the distal edge of the Indian passive margin rather than within Neotethys. Hence, if the Transhimalayan trench was incompletely filled and represented a barrier to turbidites derived from Asia, then the IAPR should necessarily coincide in time with collision onset, which in the Mubala section would thus be robustly constrained between 62.7 Ma (youngest ages of detrital zircon in the oldest Asian-derived sandstone) and 61.0 ± 0.3 Ma (age of the tuff ~30 m above the IAPR).

The superposition of Asian-derived turbidites onto Indian-derived turbidites in the Mubala section, however, may have occurred somewhat earlier than actual collision onset. The Transhimalayan trench may have been overfilled, and thus bypassed by turbiditic flows spreading oceanward and reaching the edge of the Indian continental margin at some distance within the Neotethys. In the heavily sediment-filled trench of south-central Chile, for instance, turbiditic deposits extend as far as 250 km seaward of the trench axis (Contreras-Reyes et al., 2010). Considering the rapid convergence rate of India and Asia in the early Paleocene (150 km/Ma, Copley et al., 2010), even in such an overfilled-trench scenario the onset of continental collision should be quite close to 61 Ma.

8. The Discrepancy with Paleolatitude Data

Plate circuit reconstructions suggest that >4,000 km of India-Asia convergence took place since 60 Ma, whereas the estimated upper-crustal shortening amounts to only ~2000 km. Such a discrepancy led to hypothesizing a series of putative basins apt to somehow "fill the gap" (e.g., Greater India basin of van Hinsbergen et al., 2012; Xigaze backarc basin of Kapp & DeCelles, 2019; north India sea of Yuan et al., 2021). Sandstones from the Denggang Formation, however, containing detritus from the Deccan Traps and the underlying strata indicate sediment transport from India and the Tethyan Himalaya, precluding the existence of an oceanic basin to the south. An oceanic basin for which, anyway, no geological evidence was ever reported. We agreed with the statement by Kapp and DeCelles (2019) that "all existing interpretations present challenges—we are missing evidence for either a large amount of Cenozoic shortening in the Himalaya and Asia or one or more Cenozoic suture zones." The paleolatitude controversy cannot be solved at the desk by imagining the existence of oceanic basins in the absence of any field-related geological evidence. It thus stands open. The key to solve the discrepancy we suggest should be from the paleomagnetic method itself, not the re-interpretation of the geological data.

9. Conclusion

The Mubala section consists of turbiditic and abyssal sediments deposited onto the Indian continental rise (Denggang and lower Sangdanlin formations) and in the Transhimalayan trench (upper Sangdanlin and Zheya formations). Several provenance changes are recorded in the Denggang and lower Sangdanlin formations, indicating erosion of the Indian shield and its cover strata before, during, and after the major outburst of Deccan continental flood basalts. The major provenance reversal from India to Asia occurred at the boundary between the lower and upper Sangdanlin Formation, and is robustly bracketed between 62.7 Ma (youngest detrital zircon in the oldest Asian-derived sandstone) and 61.0 ± 0.3 Ma (age of the tuff intercalated ~30 m above). If the Mubala turbidites were not deposited far away from the overfilled Transhimalayan trench, then our data indicate that the continental margins of India and Asia first engaged in collision very close to 61 Ma (early Selandian) in this part of the Himalaya. This represents the most precise direct age constraint ever obtained on the age of the India-Asia collision to date.

Data Availability Statement

Supporting figures and data are provided in Figures S1–S3 and Tables S1–S6, which can be found at website https://osf.io/bcjy3/.

Acknowledgments
The authors thank Hanpu Fu, Weiqiang Ji, and Xiaoping Xia for their assistance in the field and in the laboratory, Mara Limonta and Wendong Liang for heavy-mineral analyses, and Heinrich Bahlburg and Fuyuan Wu for fruitful discussions. The authors are also grateful to Prof. Peter DeCelles, Dr. Devon Orme and Dr. Christopher Spencer for their insightful and constructive comments. This study was supported financially by the National Science Foundation of China (projects 41525007, 91755209, 41972106), the State Key Laboratory of Mineral Deposits Research, Nanjing University (2018-LAMD-K01) and China Postdoctoral Science Foundation (Grant No. 2019M662136).

References

Aitchison, J. C., Ali, J. R., & Davis, A. M. (2007). When and where did India and Asia collide? *Journal of Geophysical Research*, *112*, B05423. https://doi.org/10.1029/2006JB004706

An, W., Hu, X., & Garzanti, E. (2017). Sandstone provenance and tectonic evolution of the Xiukang Mélange from Neotethyan subduction to India-Asia collision (Yarlung-Zangbo suture). *Gondwana Research*, *41*, 222–234.

An, Z., Kutzbach, J. E., Prell, W. L., & Porter, S. C. (2001). Evolution of Asian monsoons and phased uplift of the Himalaya–Tibetan plateau since Late Miocene times. *Nature*, *411*(6833), 62–66.

Beck, R. A., Burbank, D. W., Sercombe, W. J., Riley, G. W., Barndt, J. K., Berry, J. R., et al. (1995). Stratigraphic evidence for an early collision between northwest India and Asia. *Nature*, *373*(6509), 55–58.

Cawood, P., Johnson, M., & Nemchin, A. (2007). Early Palaeozoic orogenesis along the Indian margin of Gondwana: Tectonic response to Gondwana assembly. *Earth and Planetary Science Letters*, *255*, 70–84.

Chenet, A., Quidelleur, X., Fluteau, F., Courtillot, V., & Bajpai, S. (2007). $^{40}K–^{40}Ar$ dating of the Main Deccan large igneous province: Further evidence of KTB age and short duration. *Earth and Planetary Science Letters*, *263*(1–2), 1–15.

Contreras-Reyes, E., Flueh, E. R., & Grevemeyer, I. (2010). Tectonic control on sediment accretion and subduction off south-central Chile. *Tectonics*, *29*(6), TC6018. https://doi.org/10.1029/2010TC002734

Copley, A., Avouac, J.-P., & Royer, J.-Y. (2010). India-Asia collision and the Cenozoic slowdown of the Indian plate: Implications for the forces driving plate motions. *Journal of Geophysical Research*, *115*, B03410. https://doi.org/10.1029/2009JB006634

DeCelles, P. G., Gehrels, G. E., Quade, J., LaReau, B., & Spurlin, M. (2000). Tectonic implications of U-Pb zircon ages of the Himalayan orogenic belt in Nepal. *Science*, *288*, 497–499.

DeCelles, P. G., Kapp, P., Gehrels, G. E., & Ding, L. (2014). Paleocene-Eocene foreland basin evolution in the Himalaya of southern Tibet and Nepal: Implications for the age of initial India-Asia collision. *Tectonics*, *33*(5), 824–849.

DeCelles, P. G., Leary, R. J., & Kapp, P. (2018). Cenozoic basin evolution in the Indus-Yarlung suture zone and High Himalaya. In R. V. Ingersoll, T. F. Lawton, & S. A. Graham (Eds.), Tectonics, sedimentary basins, and provenance: A celebration of William R. Dickinson's career, geological society of America special papers (Vol. 540, pp. 1–33). Boulder, CO: Gelogical Society of America.

Ding, L., Kapp, P., & Wan, X. (2005). Paleocene-Eocene record of ophiolite obduction and initial India-Asia collision, south central Tibet. *Tectonics*, *24*(3), TC3001. https://doi.org/10.1029/2004TC001729

Garzanti, E. (2008). Comment on "When and where did India and Asia collide?" by Jonathan C. Aitchison, Jason R. Ali, and Aileen M. Davis. *Journal of Geophysical Research*, *113*, B04411. https://doi.org/10.1029/2007JB005276

Garzanti, E. (2019). Petrographic classification of sand and sandstone. *Earth-Science Reviews*, *192*, 545–563.

Garzanti, E., Baud, A., & Mascle, G. (1987). Sedimentary record of the Northward flight of India and its collision with Eurasia (Ladakh Himalaya, India). *Geodinamica Acta*, *1*(4–5), 297–312.

Garzanti, E., & Hu, X. (2015). Latest cretaceous Himalayan tectonics: Obduction, collision or Deccan-related uplift? *Gondwana Research*, *28*(1), 165–178. https://doi.org/10.1016/j.gr.2014.03.010

Gehrels, G., Kapp, P., DeCelles, P., Pullen, A., Blakey, R., Weislogel, A., et al. (2011). Detrital zircon geochronology of pre-Tertiary strata in the Tibetan-Himalayan orogen. *Tectonics*, *30*(5), TC5016. https://doi.org/10.1029/2011TC002868

Hu, X., An, W., Garzanti, E., & Liu, Q. (2020). Recognition of trench basins in collisional orogens: Insights from the Yarlung Zangbo suture zone in southern Tibet. *Science China Earth Sciences*, *63*, 2017–2028.

Hu, X., An, W., Wang, J., Garzanti, E., & Guo, R. (2014). Himalayan detrital chromian spinels and timing of Indus-Yarlung ophiolite erosion. *Tectonophysics*, *621*, 60–68.

Hu, X., Garzanti, E., & An, W. (2015). Provenance and drainage system of the Early Cretaceous volcanic detritus in the Himalaya as constrained by detrital zircon geochronology. *Journal of Palaeogeography*, *4*(1), 85–98.

Hu, X., Garzanti, E., Moore, T., & Raffi, I. (2015). Direct stratigraphic dating of India-Asia collision onset at the Selandian (middle Paleocene, 59 ± 1 Ma). *Geology*, *43*(10), 859–862.

Hu, X., Garzanti, E., Wang, J., Huang, W., An, W., & Webb, A. (2016). The timing of India-Asia collision onset—facts, theories, controversies. *Earth-Science Reviews*, *160*, 264–299.

Hu, X., Jansa, L., Chen, L., Griffin, W. L., O'Reilly, S. Y., & Wang, J. G. (2010). Provenance of Lower Cretaceous Wolong Volcaniclastics in the Tibetan Tethyan Himalaya: Implications for the final breakup of Eastern Gondwana. *Sedimentary Geology*, *223*(3–4), 193–205.

Hu, X., Sinclair, H. D., Wang, J., Jiang, H., & Wu, F. (2012). Late Cretaceous-Palaeogene stratigraphic and basin evolution in the Zhepure Mountain of southern Tibet: Implications for the timing of India-Asia initial collision. *Basin Research*, *24*(5), 520–543.

Ingersoll, R. V., Fullard, T. F., Ford, R. L., Grimm, J. P., Pickle, J. D., & Sares, S. W. (1984). The effect of grain size on detrital modes; a test of the Gazzi-Dickinson point-counting method. *Journal of Sedimentary Research*, *54*(1), 103–116.

Ji, W. Q., Wu, F. Y., Chung, S. L., Li, J. X., & Liu, C. Z. (2009). Zircon U–Pb geochronology and Hf isotopic constraints on petrogenesis of the Gangdese batholith, southern Tibet. *Chemical Geology*, *262*(3–4), 229–245.

Kamenetsky, V. S., Crawford, A. J., & Meffre, S. (2001). Factors controlling chemistry of magmatic spinel: An empirical study of associated Olivine, Cr-spinel and melt inclusions from primitive rocks. *Journal of Petrology*, *42*(4), 655–671.

Kapp, P., & Decelles, P. (2019). Mesozoic-Cenozoic geological evolution of the Himalayan-Tibetan orogen and working tectonic hypotheses. *American Journal of Science*, *319*, 159–254.

Leech, M. L., Singh, S., Jain, A. K., Klemperer, S. L., & Manickavasagam, R. M. (2005). The onset of India-Asia continental collision: Early, steep subduction required by the timing of UHP metamorphism in the western Himalaya. *Earth and Planetary Science Letters*, *234*(1–2), 83–97.

Li, J., Hu, X., Garzanti, E., Banerjee, S., & BouDagher Fadel, M. (2020). Late Cretaceous topographic doming caused by initial upwelling of Deccan magmas: Stratigraphic and sedimentological evidence. *The Geological Society of America Bulletin*, *132*(3–4), 835–849.

Li, X., Wang, C., & Hu, X. (2005). Stratigraphy of deep-water Cretaceous deposits in Gyangze, southern Tibet, China. *Cretaceous Research*, *26*(1), 33–41.

Li, Y., Wang, C., Hu, X., Bak, M., Wang, J., & Chen, L. (2007). Characteristics of Early Eocene radiolarian assemblages of the Saga area, southern Tibet and their constraint on the closure history of the Tethys. *Chinese Science Bulletin*, *52*(12), 2108–2114.

Metcalf, K., & Kapp, P. (2017). The Yarlung suture mélange, Lopu Range, southern Tibet: Provenance of sandstone blocks and transition from oceanic subduction to continental collision. *Gondwana Research*, *48*, 15–33.

Mutti, E., Davoli, G., Petroli, A., & Geologia, U. (1992). *Turbidite sandstones: Agip, Istituto di geologia*. Università di Parma.

Najman, Y., Appel, E., Boudagher-Fadel, M., Bown, P., Carter, A., Garzanti, E., et al. (2010). Timing of India-Asia collision: Geological, biostratigraphic, and paleomagnetic constraints. *Journal of Geophysical Research*, *115*, B12416. https://doi.org/10.1029/2010jb007673

Najman, Y., Jenks, D., Godin, L., Boudagher-Fadel, M., Millar, I., Garzanti, E., et al. (2017). The Tethyan Himalayan detrital record shows that India–Asia terminal collision occurred by 54 Ma in the Western Himalaya. *Earth and Planetary Science Letters*, *459*, 301–310.

Orme, D. A., Carrapa, B., & Kapp, P. (2014). Sedimentology, provenance and geochronology of the upper Cretaceous-lower Eocene western Xigaze forearc basin, southern Tibet. *Basin Research*, *27*, 387–411.

Orme, D. A., Laskowski, A. K., Zilinsky, M. F., Chao, W., Guo, X., Cai, F., & Lin, D. (2021). Sedimentology and provenance of newly identified late Cretaceous trench-basin strata, Dênggar, southern Tibet: Implications for development of the Eurasian margin prior to India-Asia collision. *Basin Research*. https://doi.org/10.1111/BRE.12521

Pan, G., Ding, J., Yao, D., & Wang, L. (2004). *The guide book of 1:1,500,000 geologic map of the Qinghai-Xizang (Tibet) Plateau and adjacent areas*. Chengdu: Chengdu Map Publishing Company.

Ravizza, G. E., & Zachos, J. C. (2014). Records of Cenozoic ocean chemistry. In H. D. Holland, & K. K. Turekian (Eds.), Treatise on geochemistry (2nd ed., Vol. 8, pp. 543–568). Amsterdam: Elsevier Science.

Sciunnach, D., & Garzanti, E. (2012). Subsidence history of the Tethys Himalaya. *Earth-Science Reviews*, *25*, 179–198.

van Hinsbergen, D. J., Lippert, P. C., Dupont-Nivet, G., McQuarrie, N., Doubrovine, P. V., Spakman, W., & Torsvik, T. H. (2012). Greater India Basin hypothesis and a two-stage Cenozoic collision between India and Asia. *Proceedings of the National Academy of Sciences*, *109*(20), 7659–7664.

Wang, J., Hu, X., Jansa, L., & Huang, Z. (2011). Provenance of the upper cretaceous–Eocene deep-water sandstones in Sangdanlin, southern Tibet: Constraints on the timing of initial India-Asia collision. *The Journal of Geology*, *119*(3), 293–309.

Willems, H., Zhou, Z., Zhang, B., & Grafe, K. U. (1996). Stratigraphy of the upper cretaceous and lower tertiary strata in the Tethyan Himalayas of Tibet (Tingri area, China). *Geologische Rundschau*, *85*(4), 723–754.
Wu, F. Y., Ji, W., Wang, J., Liu, C., Chung, S., & Clift, P. D. (2014). Zircon U–Pb and Hf isotopic constraints on the onset time of India-Asia collision. *American Journal of Science*, *314*(2), 548–579.
Yin, A., & Harrison, T. M. (2000). Geologic evolution of the Himalayan-Tibetan orogen. *Annual Review of Earth and Planetary Sciences*, *28*(1), 211–280.
Yuan, J., Yang, Z., Deng, C., Krijgsman, W., Hu, X., Li, S., et al. (2021). Rapid drift of the Tethyan Himalaya terrane before two-stage India-Asia collision. *National Science Review*. https://doi.org/10.1093/nsr/nwaa173

References From the Supporting Information

Andersen, T. (2002). Correction of common lead in U–Pb analyses that do not report 204Pb. *Chemical Geology*, *192*(1–2), 59–79.
An, W., Hu, X., Garzanti, E., BouDagher-Fadel, M. K., Wang, J., & Sun, G. (2014). Xigaze forearc basin revisited (South Tibet): Provenance changes and origin of the Xigaze Ophiolite. *The Geological Society of America Bulletin*, *126*, 1595–1613.
Garzanti, E., & Andò, S. (2007). Heavy mineral concentration in modern sands: Implications for provenance interpretation. In M. A. Mange, & D. T. Wright (Eds.), Developments in sedimentology (Vol. 58, pp. 517–545). Elsevier.
Griffin, W. L., Pearson, N. J., Belousova, E. A., & Saeed, A. (2007). Reply to "Comment to short-communication 'Comment: Hf-isotope heterogeneity in zircon 91500 by W. L. Griffin, N. J. Pearson, E. A. Belousova, & A. Saeed. *Chemical Geology*, *244*, 354–356.
Griffin, W. L., Powell, W. J., Pearson, N. J., & O'Reilly, S. Y. (2008). GLITTER: Data reduction software for laser ablation ICP–MS. In P. Sylvester (Ed.), Laser ablation–ICP–MS in the earth sciences: Current practices and outstanding issues (Vol. 40, pp. 308–311). Quebec: Mineralogical Association of Canada.
Horstwood, M., Košler, J., Gehrels, G., Jackson, S., McLean, N., Paton, C., et al. (2016). Community-derived standards for LA-ICP-MS U-(Th-)Pb Geochronology—Uncertainty propagation, age interpretation and data reporting. *Geostandards and Geoanalytical Research*, *40*, 311–332.
Li, X.-H., Liu, Y., Li, Q.-L., Guo, C.-H., & Chamberlain, K. R. (2009). Precise determination of Phanerozoic zircon Pb/Pb age by multicollector SIMS without external standardization. *Geochemistry, Geophysics, Geosystems*, *10*(4), Q04010. https://doi.org/10.1029/2009GC002400
Li, X., Tang, G., Gong, B., Yang, Y., Hou, K., Hu, Z., et al. (2013). Qinghu zircon: A working reference for microbeam analysis of U–Pb age and Hf and O isotopes. *Chinese Science Bulletin*, *58*, 4647–4654.
Mange, M. A., & Maurer, H. F. W. (1992). *Heavy minerals in color*. London, UK: Chapman and Hall.
Scherer, E., Munker, C., & Mezger, K. (2001). Calibration of the lutetium-hafnium clock. *Science*, *293*, 683–687.
Sláma, J., Košler, J., Condon, D., Crowley, J., Gerdes, A., Hanchar, J., et al. (2008). Plešovice zircon—A new natural reference material for U–Pb and Hf isotopic microanalysis. *Chemical Geology*, *249*, 1–35.
Wang, J., Hu, X., Garzanti, E., An, W., & Liu, X. (2017). The birth of the Xigaze forearc basin in southern Tibet. *Earth and Planetary Science Letters*, *465*, 38–47. https://doi.org/10.1016/j.epsl.2017.02.036
Wiedenbeck, M., Alle, P., Corfu, F., Griffin, W. L., Meier, M., Oberli, F., et al. (1995). Three natural Zircon standards for U-Th-Pb, Lu-Hf, trace element and REE analyses. *Geostandards Newsletter*, *19*(1), 1–23. https://doi.org/10.1111/j.1751-908X.1995.tb00147.x
Wu, F. Y., Ji, W. Q., Liu, C. Z., & Chung, S. L. (2010). Detrital zircon U–Pb and Hf isotopic data from the Xigaze fore-arc basin: Constraints on Transhimalayan magmatic evolution in southern Tibet. *Chemical Geology*, *271*(1–2), 13–25.
Xie, L., Zhang, Y., Zhang, H., Sun, J., & Wu, F. (2008). In situ simultaneous determination of trace elements, U–Pb and Lu–Hf isotopes in zircon and badde-leyite. *Chinese Science Bulletin*, *53*, 1565–1573.